RSC Advances

PAPER

View Article Online
View Journal | View Issue

Cite this: *RSC Adv.*, 2019, **9**, 9211

Polyaniline/chitosan as a corrosion inhibitor for mild steel in acidic medium

Peipei Kong,[ab] Huixia Feng,*[ab] Nali Chen,[ab] Yong Lu,[ab] Shiyou Li[ab] and Peng Wang[ab]

Received 8th January 2019
Accepted 8th March 2019

DOI: 10.1039/c9ra00029a

rsc.li/rsc-advances

The inhibition performance of polyaniline (PANI)/chitosan (CTS) on metal corrosion in 0.5 M HCl was studied using electrochemical measurements, quantum chemical calculations and morphological observations. Potentiodynamic polarization measurements show that PANI/CTS acts essentially as a mixed-type inhibitor. The inhibition efficiency increases and corrosion rates decrease with increasing concentrations of PANI/CTS. The relationship between experimental inhibition efficiency and quantum chemical calculations that were developed to describe the corrosion inhibition process are discussed.

1 Introduction

Metals are used for numerous applications in modern society; however, metals often undergo corrosion in acidic environments, which can lead to their failure. Consequently, many researchers worldwide have explored the development of more reliable methods and strategies to prevent or minimize acid corrosion. A number of references have reported carbohydrate polymers and conducting polymers as efficient corrosion inhibitors that are used as preventative measures for numerous industrial and construction applications.[1,2]

Recently, chitosan has received increasing attention as a natural material that displays excellent biocompatibility, biodegradability, good adhesion and nontoxic properties.[3,4] Chitosan contains electron-rich hydroxyl and amino groups whose lone pair electrons form strong coordination bonds to the metal surface, which enable them to function as corrosion inhibitors.[5] Some authors have described the inhibition performance of chitosan and its derivatives on metal corrosion in acidic media. El-Haddad[6] studied chitosan as a green inhibitor for copper corrosion and indicated that it possessed good inhibition efficiency in 0.5 M HCl. Our previous work prepared salicylaldehyde-modified chitosan and studied the effect of the inhibitor on Q235 steel in 1.0 M HCl solution by a weight loss method and electrochemical technology. The inhibitor exhibited excellent anticorrosion performance.[7] Polyaniline (PANI) is a conducting polymer that has been used as a promising eco-friendly corrosion inhibitor. It is easy to prepare at low cost and exhibits good electrical conductivity and low toxicity and has a fully reversible redox cycle.[8] A number of studies have indicated that PANI is a good candidate as an inhibitor for preventing steel corrosion in acid. Rania E. *et al.*[9] studied un-doped polyaniline and self-doped polyaniline for carbon steel corrosion inhibition behaviour in 1.0 M HCl and showed that both compounds can be effectively used as corrosion inhibitors. Yi Y. *et al.*[10] showed that conducting polyaniline as a corrosion inhibitor for mild steel plays an important role in retaining efficiency. A previous study revealed that chitosan and PANI are efficient inhibitors to protect steel in acidic solution. Bao R. H. *et al.*[11] reported carboxymethyl chitosan doped polyaniline as an inhibitor for mild steel where it behaved as a mixed-type inhibitor with excellent inhibition efficiency. However, the preparation process of carboxymethyl chitosan-doped polyaniline is complicated, and its corrosion inhibition mechanism has not been studied. We found that few related studies have reported the corrosion mechanism of PANI/CTS composites.

Based on the analysis above, this work successfully prepared a PANI/CTS composite by an effective one-pot synthesis route. Different techniques were employed, such as potentiodynamic polarization and impedance spectroscopy (EIS), to investigate how PANI/CTS additives prevent corrosion of Q235 steel in 0.5 M HCl. The metal surface morphological features were evaluated using scanning electron microscopy (SEM). The molecular structure of the composite was identified by Fourier transform infrared spectroscopy (FTIR). The inhibition mechanism was interpreted using quantum chemical techniques.

2 Experimental

2.1 Materials

Aniline (An, analytically pure) and chitosan (medium molecular weight) were obtained from Aldrich Chemical Co. Ltd, and the aniline was distilled under reduced pressure prior to use. Ammonium persulfate [$(NH_4)_2S_2O_8$, APS] and aminosulfonic

[a]State Key Laboratory of Advanced Processing and Recycling of Nonferrous Metals, Lanzhou University of Technology, Lanzhou 730050, China. E-mail: fenghx66@163.com; Tel: +86-931-2973301

[b]College of Petrochemical Technology, Lanzhou University of Technology, Lanzhou 730050, China

acid (NH_2SO_3H) were purchased from Tianjin Daming Chemical Co. Ltd. AR grade acetic acid, acetone and ethanol were used as received.

2.2 Synthesis of polyaniline/chitosan composite

A polyaniline/chitosan composite (PANI/CTS) was synthesized in CH_3COOH and NH_2SO_3H media. The synthesis route is illustrated in Fig. 1. An aqueous solution of chitosan (0.2 g) was obtained by dissolving it in 40 mL of 0.33 M acetic acid for 24 h, and 12 mmol of polyaniline monomer was dissolved in 20 mL of 0.8 M NH_2SO_3H. This polyaniline solution was added to the chitosan solution and stirred for 30 min to form a homogeneous solution. An ammonium persulfate (10 mmol) solution was prepared by dissolving in 0.33 M CH_3COOH, which was then added dropwise to a homogeneous solution for 1 h at 0–5 °C. The molar ratio of oxidant to monomer was 1 : 2, with the polymerization reaction carried out at 0–5 °C for 6 h. The precipitated composite was collected by filtering and washing with water and ethanol, respectively, and then dried at 50 °C for 12 h in a vacuum oven.

2.3 Electrochemical measurements

Electrochemical measurements were performed in a typical three-electrode electrochemical cell using a CHI660E electrochemical workstation. Test metal samples used for electrochemical experiments were machined into rectangular specimens and then embedded in polytetrafluoroethylene (PTFE) with an exposed geometrical circular area of 1 cm^2. The metal samples served as a working electrode (WE), with a platinum foil used as the counter electrode (PE) and a saturated calomel electrode (SCE) as the reference electrode (RE). Potentiodynamic polarization experiments were carried using a potential of −800 to 200 mV for a scan rate of 1.0 mV s^{-1}, with all potentials reported in mV (SCE). EIS measurements were carried out over a frequency range of 0.01 to 100 kHz with an AC voltage amplitude of 5.0 mV using an open circuit potential. Measurements were performed in naturally aerated and unstirred solutions after samples had been exposed to corrosive media at room temperature for 2 h. ZSimpWin software was used to fit and analyse data produced from the EIS measurements. Experimental results were carried out three times, with good reproducibility observed in all cases.

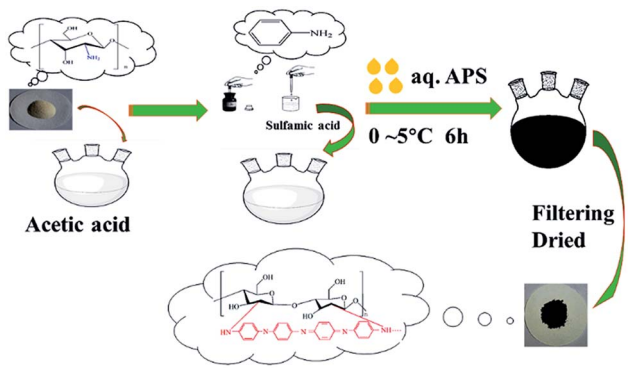

Fig. 1 Illustration of the preparation process of the PANI/CTS composite.

2.4 Metal surface and inhibitor characterization

Morphological studies of the mild steel samples were undertaken by SEM examination of surfaces exposed to different test solutions using a scanning electron microscope (SEM, S-4300, Hitachi Co., Ltd. Tokyo, Japan). The molecular structure of the samples was identified by Fourier transform infrared spectroscopy (FTIR, JRT-7000; JASCO, Japan).

2.5 Quantum chemical study

Quantum chemical calculations were carried out using density functional theory (DFT) with a 6-31G(d,p) basis set to describe all atoms using a Gaussian 09 program.[12] Energies of the highest occupied molecular orbital E_{HOMO}, the lowest unoccupied molecular orbital E_{LUMO}, the energy gap ΔE between E_{LUMO} and E_{HOMO}, and Mulliken charges on the backbone atoms of PANI/CTS molecule were calculated using Gauss View.

3 Results and discussion

3.1 Characterization of PANI/CTS inhibitor

The FTIR spectra of the chitosan and PANI/CTS composite are shown in Fig. 2. The spectrum of chitosan showed a band at 1602 cm^{-1} for $-NH_2$ bending.[13–19] The spectrum showed a band at 1260 cm^{-1} that could be attributed to the saccharide structure.[20] The absorption band at 1156 cm^{-1} was assigned to the anti-symmetric stretching of C–O–C bridges, with C–O stretching vibrations present at 1066 cm^{-1}.[15,21,22] The spectrum of PANI revealed peaks at 1596 and 1483 cm^{-1} corresponding to characteristic C–C stretching of its quinonoid and benzenoid rings, respectively.[23,24] The peak at 1295 was attributed to C–N and C=N stretching vibrations.[25]

The FTIR spectrum of the PANI/CTS composite showed all the characteristic bands that were present in the separate IR spectra of chitosan and polyaniline. The band at 1640 cm^{-1} was characteristic of a nitrogen quinone (Q) structure, with a 1472 cm^{-1} band corresponding to a benzene ring (B) structure. Bands at 1295 and 1108 cm^{-1} were assigned to C–N stretching and N=Q=N stretching, respectively, with a peak at 795 cm^{-1} attributed to out-of-plane C–H stretching.[15,17,26,27] Some of the FTIR absorptions for the PANI/CTS composite were shifted to shorter wavenumbers, whereas other bands were shifted to longer wavenumbers. These FTIR results indicated that a series of electrostatic forces and hydrogen bonding interactions resulted in the successful formation of a PANI/CTS composite.[28]

3.2 Potentiodynamic polarization

Kinetics of the cathodic and anodic reactions occurring at the Q235 steel electrode in 0.5 M HCl solution were determined using potentiodynamic polarization measurements at room temperature in the absence and presence of different concentrations of PANI/CTS. A steady-state potential was attained after 0.5 h due to the rapid dissolution of Q235 steel by the acidic medium. Fig. 3 shows the effect of increasing PANI/CTS

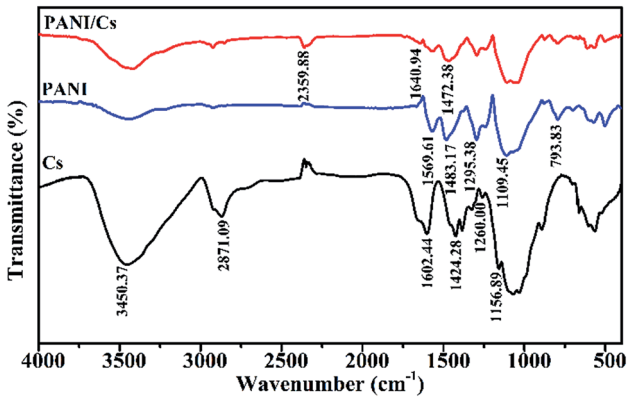

Fig. 2 FTIR spectra of chitosan (CTS), PANI and the PANI/CTS composite.

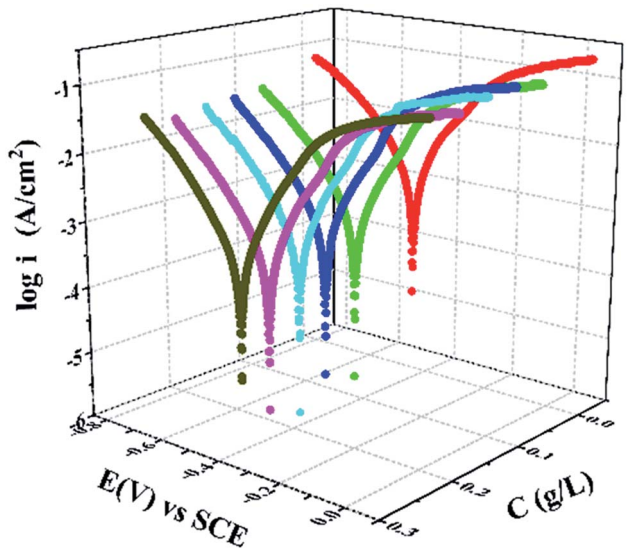

Fig. 3 Potentiodynamic polarization curves for Q235 steel samples in 0.5 M HCl in the absence and presence of different concentrations of PANI/CTS inhibitor.

concentrations on the cathodic and anodic polarization curves of Q235 steel, which revealed a decrease in corrosion rate for increasing PANI/CTS concentrations. Corrosion current densities (i_{corr}), corrosion potentials (E_{corr}), polarization resistances (R_P), anodic and cathodic Tafel slopes and inhibition efficiency ($\eta\%$) were calculated from the polarization curves shown in Table 1. Inhibition efficiency ($\eta\%$) and corrosion rate (C_R) values were calculated using eqn (1) and (2):

$$\eta\% = (i^0_{corr} - i_{corr})/i^0_{corr} \times 100 \quad (1)$$

$$C_R = \{(3.286 \times 10^{-3}) \times (i_{corr} \times M_{Fe})\}/np \quad (2)$$

where (i_{corr}) and (i^0_{corr}) are the corrosion current density with and without inhibitor, respectively, M_{Fe} is the molecular weight of steel, n is the number of electrons transferred in the corrosion reaction, and p is the density of the specimen (7.86 g cm^{-3}). Table 1 reports values for anodic Tafel slopes (b_a) and cathodic Tafel slopes (b_c) for hydrogen evolution, where θ is the degree of surface coverage ($\theta = \eta\%/100$).[29]

Polarization curves indicated that both anodic metal dissolution and cathodic hydrogen evolution reactions were affected by the addition of PANI/CTS, with the parallel nature of the Tafel lines suggesting that an activation-controlled hydrogen evolution reaction was occurring.[30,31] Changes to the E_{corr} value were less than 85 mV, providing evidence that the PANI/CTS inhibitor functioned as a mixed-type inhibitor that shifted in a positive direction for increased inhibitor concentration.[32] I_{corr} values were found to decrease for increased PANI/CTS concentrations, which was due to a greater fraction of the steel surface being covered.[33–36] Increasing the concentration of PANI/CTS resulted in decreased corrosion rates due to more reaction sites on the steel surface inhibitor being covered through a geometric blocking process.[37]

3.3 EIS measurements

Electrochemical impedance spectroscopy was used to study the nature of the electrochemical processes to provide mechanistic information on the influence of PANI/CTS on the metal dissolution process at the mild steel/0.5 M HCl interface. Fig. 4a shows impedance spectra for varying concentrations of PANI/CTS inhibitor, with impedance levels changing significantly after the samples were immersed in PANI/CTS solution for 2 h. Nyquist plots revealed a single depressed capacitive loop over the frequency range that was studied, with the semicircles indicating the charge-transfer resistant, double-layer capacitance properties of the electrode.[38–41] The single semicircle in

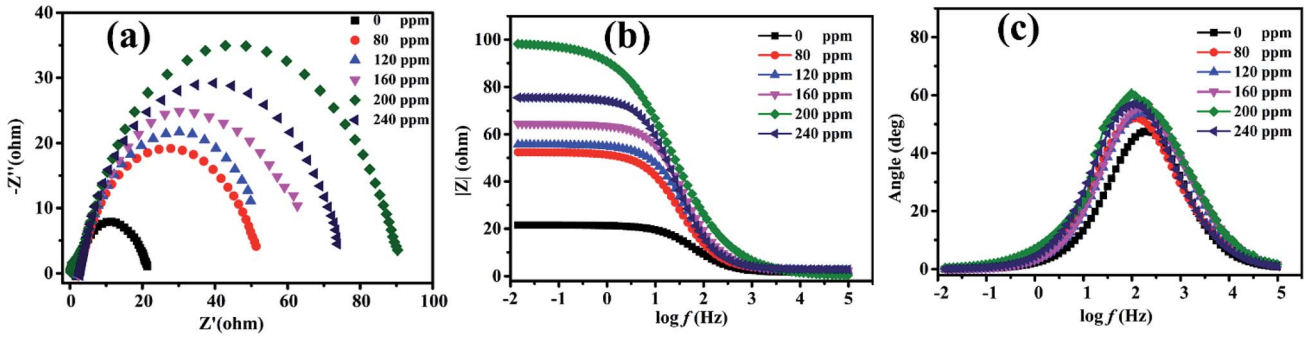

Fig. 4 (a) Impedance curves, (b) Bode plots and (c) phase angle plot of PANI/CTS.

Table 1 Polarization parameters for Q235 steel in 0.5 M HCl in the absence and presence of inhibitor at room temperature

Con (ppm)	b_a (mV per decade)	b_c (mV per decade)	i_{corr} (A cm^{-2})	R_P (Ω cm^2)	E_{corr} (V *vs.* SCE)	η (%)
Blank	7.665	7.229	1.249×10^{-3}	2.3	−0.4486	—
80	8.849	7.523	4.107×10^{-4}	6.5	−0.4728	67.12
120	8.815	7.209	3.734×10^{-4}	7.3	−0.4819	70.10
160	9.300	7.112	3.658×10^{-4}	7.2	−0.4736	70.71
200	9.442	7.190	2.620×10^{-4}	10	−0.4680	79.02
240	9.553	7.273	3.508×10^{-4}	7.4	−0.4726	71.91

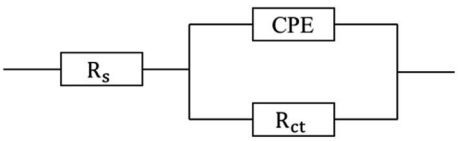

Fig. 5 Equivalent circuit used to fit experimental data in the presence of PANI/CTS.

the Nyquist diagram indicated that metal dissolution was controlled by a single transfer process, with similar shaped Nyquist plots indicating that the corrosion mechanism was unaffected in the presence of inhibitor molecules.[42,43] The Nyquist diagrams for Q235 steel in the presence of the PANI/CTS composite revealed that the diameter of the semicircles was larger than those produced in its absence. This increase in diameter indicated increased corrosion resistance of Q235 steel, with adsorption of the PANI/CTS inhibitor on its surface resulting in double layer charging effects that produce faradaic impedance processes at the reaction interface.[44–46] Fig. 4(b and c) represents the corresponding Bode and phase angle plots of PANI/CTS, respectively.

It is noted that, along with the addition and increasing inhibitor concentration in the solution, the frequency ranges with the maximum phase angle and the low-frequency impedance values increased, showing effective adsorption of inhibitor molecules on the Q235 steel surface.[47,48]

The steel corrosion mechanism was investigated in detail using an equivalent circuit model, which provided information about the interface reaction in the corrosive medium.[48] Electrochemical impedance parameters were determined by fitting the impedance spectra, which enabled constant phase element (CPE), solution resistance (R_s) and charge transfer resistance (R_{ct}) values to be obtained. Using the CPE value as a substitute for the capacitance value (C_{dl}) enabled the impedance behaviour of the electric double layer to be accurately determined. The equivalent circuit and the parameters that were used to fit the impedance data from corrosion experiments are shown in Fig. 5 and Table 2.

Inhibition efficiency (η%) values were calculated from R_{ct} values using eqn (3):[49]

$$\eta\% = (R_{ct} - R_{ct}^0)/R_{ct} \times 100 \quad (3)$$

where R_{ct}^0 and R_{ct} are the charge-transfer resistance in the absence/presence of inhibitor, respectively. The R_{ct} values of the inhibited systems were higher than for the non-inhibited system, which was due to a reduction in metal dissolution caused by the inhibitor adsorbing to the steel surface. Electrode n values were determined to be between 0.8–10, indicating that their metal surfaces were rough and non-homogeneous,[50,51] and an increase in inhibitor concentration resulted in improved corrosion resistance.

3.4 Surface analysis

SEM has been widely used to observe the morphological features of metal surfaces. The surface morphologies of polished Q235 steel specimens exposed to 0.5 M HCl (without PANI/CTS inhibitor and with 200 ppm PANI/CTS inhibitor) after immersion for 2 h was examined by SEM, and the results are shown in Fig. 6. The surface of the polished Q235 steel specimen appeared smooth (Fig. 6a). The surface of the Q235 steel

Table 2 Electrochemical impedance parameters for Q235 steel in 0.5 M HCl in the absence and presence of different concentrations of PANI/CTS

Con (ppm)	R_s (Ω cm^2)	Y_0 (s^n Ω^{-1} cm^{-2}) × 10^{-4}	n ($0 < n < 1$)	R_{ct} (Ω cm^2)	$C_{dl} \times 10^5$ (F cm^{-2})	η (%)
Blank	2.620	4.291	0.8544	12.41	3.631	—
80	2.574	3.018	0.8270	39.34	2.801	68.45
120	2.411	3.138	0.8131	45.58	1.832	72.77
160	2.424	1.890	0.8398	49.47	2.032	74.91
200	0.142	1.725	0.7340	81.53	3.530	84.78
240	2.853	2.248	0.8526	61.64	1.713	79.87

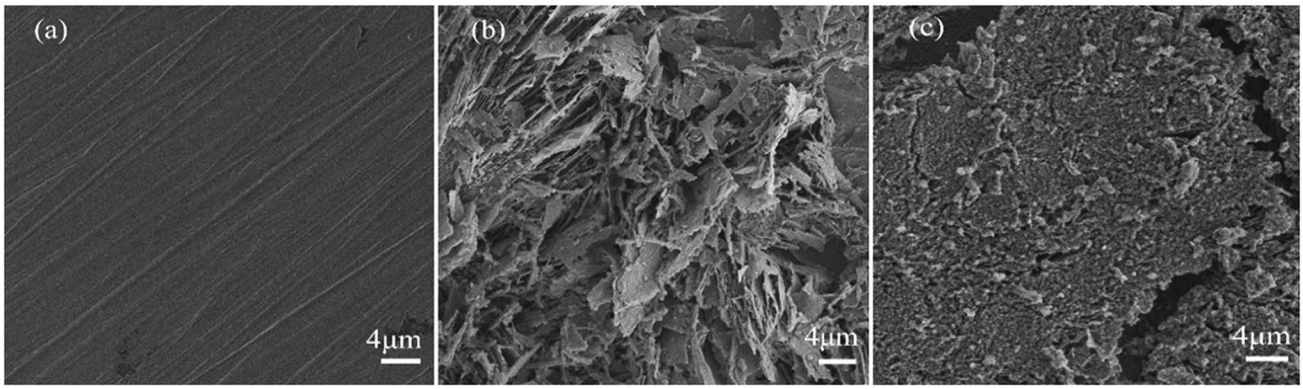

Fig. 6 SEM of (a) polished Q235 specimen, (b) Q235 specimen immersed for 2 h without PANI/CTS solution and (c) 2 h with PANI/CTS solution.

specimen exposed to 0.5 M HCl solution without PANI/CTS inhibitor (Fig. 6b) was rough, which indicated that the Q235 steel specimen was strongly corroded by the corrosion medium. In contrast, in the presence of the PANI/CTS inhibitor (Fig. 6c), there was much less damage on the Q235 steel surface, which further confirmed the formation of a protective adsorption layer. Therefore, it can be concluded that the PANI/CTS inhibitor possessed a good inhibiting ability for mild steel corrosion.

3.5 Quantum chemical calculation[52]

Frontier molecular orbital theory states that the reaction of two reagents, A and B, is determined by orbital interactions and the energy differences between their LUMO and HOMO.[53,54] The geometries of a PANI/CTS monomer were fully optimized using the Gaussian 09 software package employing a B3LYP/6-31G(d,p) method.[55] The optimized molecular structure and calculated HOMO and LUMO of the PANI/CTS molecule are shown in Fig. 7. For the HOMO of PANI/CTS, the nitrogen, oxygen atoms, –C═N groups and benzene ring of the PANI/CTS have the largest electron density with Mulliken atomic charges of −7.048 eV (10 O), −5.442 eV (12 O), −9.197 eV (14 N), −12.055 eV (26 N), −15.102 eV (38 N), and −14.912 eV (49 N). This means that N, O atoms and –C═N groups of PANI/CTS donated lone pairs of electrons and can be adsorbed on the anodic sites of the metal surface through chemical interaction with the empty d orbitals of the metal. On the other hand, the π (or p) electrons of the benzene ring (PANI) can also interact with the metal surface by sharing electrons with the metal atom, thus preventing corrosion of the steel surface.[7]

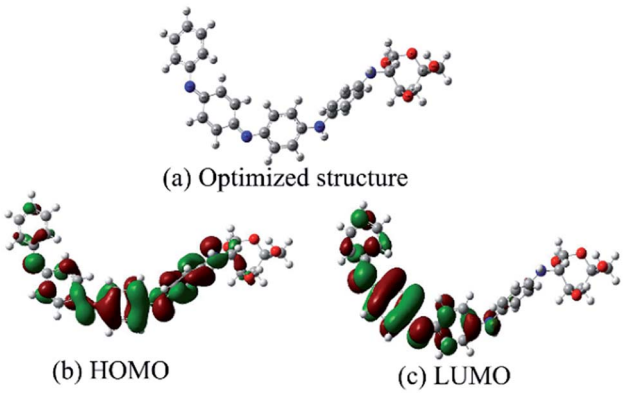

Fig. 7 Optimal molecular structure and frontier molecular orbitals (HOMO and LUMO) of PANI/CTS.

Quantum chemical values were calculated, with the energy of the highest occupied molecular orbital $E_{HOMO} = -4.645$ eV, the lowest unoccupied molecular orbital $E_{LUMO} = -2.470$ eV, a dipole moment of $\mu = 8.804$ D and an energy gap ΔE ($E_{LUMO} - E_{HOMO}$) = 2.175 eV. The high value of E_{HOMO} (−4.645 eV) likely indicates a tendency of the molecule to donate electrons to the appropriate acceptor molecule with low energy and empty molecular orbital. The value of E_{LUMO} (−2.470 eV) indicated the ability of the molecule to accept electrons. The value of ΔE provided a measure of the stability of the complex on the metal surface. Parameter μ is important for the study of the complex and its inhibitive ability. Some authors agree that a high value of μ related to the dipole–dipole interaction of the inhibitor and metal surface can enhance the adsorption strength on the metal surface, resulting in an increase of inhibition effectiveness.[56,57] Therefore, the high inhibition efficiency of a molecule can be attributed to the high dipole moment and low ΔE, which is in accordance with the inhibition efficiencies obtained above. In summary, the results of the high dipole moment and low energy gap indicated that electron transfer from PANI/CTS to the metal surface occurred during the adsorption process.

3.6 Mechanism of PANI/CTS corrosion inhibition

It is well recognized that organic inhibitor molecules inhibit metal corrosion by adsorption onto the metal/solution interface. The adsorption efficiency is affected by the molecule structure of the inhibitor, the nature and charge of the metal surface and the distribution of charge over the inhibitor molecule. Thus, a potential mechanism of organic inhibitor molecules on the metal surface can be proposed as due to the following: (a) the physisorption interactions between the protonated amine group and the negatively charged metal surface made by Cl^- anions (electrostatic), (b) the chemisorption interactions between the lone electron pair of nitrogen or

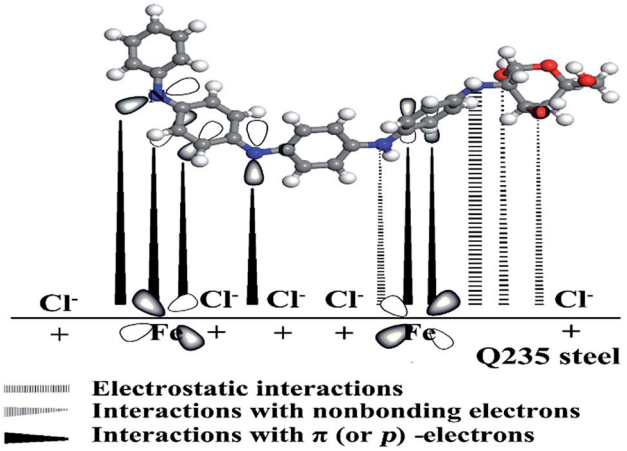

Fig. 8 A schematic diagram of the proposed inhibition mechanism of PANI/CTS on mild steel/0.5 M HCl interface.

oxygen atoms with empty d orbital of iron atoms, and (c) donor–acceptor interactions between the π (or p)-electrons of aromatic ring with vacant d orbital of iron atoms.[58]

According to the experimental results, it was clear that PANI/CTS enhanced the inhibition efficiency of mild steel in 0.5 M HCl. The reason is that PANI/CTS possessed countless repeating units (including nitrogen atoms, oxygen atoms, –C=N groups and aromatic rings).[59] In other words, the steel surface had a positive charge in the acid solution, so it was difficult for protonated PANI/CTS to approach the positively charged mild steel surface.[60] Because chloride ions have a small degree of hydration, they could attract excess negative charges around the metal interface and facilitate more positively charged inhibitor molecules. Thus, there was a synergy between adsorbed chloride ions and PANI/CTS. In addition, PANI/CTS may be adsorbed on the metal surface through the chemisorption mechanism, involving the displacement of water molecules from the mild steel surface and the sharing electrons between the N/O atoms and iron. The inhibitor molecules can also adsorb on the mild steel surface on the basis of donor–acceptor interactions between π (or p)-electrons of the aromatic ring and vacant d orbital of iron. A schematic diagram of the proposed inhibition mechanism of PANI/CTS on mild steel in 0.5 M HCl solution is shown in Fig. 8.

4 Conclusion

PANI/CTS was synthesized and evaluated for its enhanced inhibitory performance on mild steel in 0.5 M HCl. From the obtained results, the following conclusions were drawn:

(1) PANI/CTS was shown to be a good inhibitor of Q235 steel corrosion in 0.5 M HCl solution, with greater inhibition efficiency occurring for high concentrations of PANI/CTS.

(2) Polarization results revealed that PANI/CTS in 0.5 M HCl solution acted as a mixed-type inhibitor that primarily suppressed cathodic processes.

(3) EIS measurements indicated that increasing the concentration of PANI/CTS results in an increase in charge transfer resistance caused by a decrease in the overall capacitance of the system.

(4) Quantum chemical calculations suggested that the electron donating nitrogen, oxygen atoms, –C=N groups and aromatic ring of PANI/CTS are responsible for adsorption of PANI/CTS to the steel surface.

Conflicts of interest

There are no conflicts of interest to declare.

Acknowledgements

This work was supported by the Natural Science Foundation of China (grant numbers: 21664009, 51063003) and (grant numbers: 21766017, 51502124) and the Science and Technology Project of Baiyin City (grant numbers: 2017-2-11G). It acknowledges the computing resources and time of the Supercomputing Center of Cold and Arid Region Environment and Engineering Research Institute of Chinese Academy of Sciences and Supercomputing Environment of Chinese Academy of Sciences.

References

1 T. Peme, L. O. Olasunkanmi, I. Bahadur, A. S. Adekunle, M. M. Kabanda and E. E. Ebenso, *Molecules*, 2015, **20**, 16004.
2 P. P. Deshpande, E. G. Jadhav, V. J. Gelling and D. Sazou, *J. Coat. Technol. Res.*, 2014, **11**, 473.
3 N. A. Salahuddin, M. M. Ayad and M. E. Essa, *Int. J. Mater. Chem.*, 2015, **5**, 54.
4 S. John, A. Joseph, A. J. Jose and B. Narayana, *Prog. Org. Coat.*, 2015, **84**, 28.
5 S. A. Umoren and U. M. Eduok, *Carbohydr. Polym.*, 2016, **140**, 314.
6 M. N. El-Haddad, *Int. J. Biol. Macromol.*, 2013, **55**, 142.
7 N. L. Chen, P. P. Kong, H. X. Feng, Y. Y. Wang and D. Z. Bai, *Journal of Bio- and Tribo-Corrosion*, 2019, **5**, 1.
8 G. Ćirić-Marjanović, *Synth. Met.*, 2013, **177**, 1.
9 R. E. Morsi, E. A. Khamis and A. M. Al-Sabagh, *J. Taiwan Inst. Chem. Eng.*, 2016, **60**, 573.
10 Y. Yi, G. Liu, Z. Jin and D. Feng, *Int. J. Electrochem. Sci.*, 2013, **8**, 3540.
11 D. Ying, L. Hua, W. Tao, Z. Xia and H. Rong, *Acta Polym. Sin.*, 2010, **5**, 588.
12 M. J. Frisch, G. W. Trucks, H. B. Schlegel, G. E. Scuseria, M. A. Robb, J. R. Cheeseman, G. Scalmani, V. Barone, G. A. Petersson, H. Nakatsuji, X. Li, M. Caricato, A. Marenich, J. Bloino, B. G. Janesko, R. Gomperts, B. Mennucci, H. P. Hratchian, J. V. Ortiz, A. F. Izmaylov, J. L. Sonnenberg, D. Williams-Young, F. Ding, F. Lipparini, F. Egidi, J. Goings, B. Peng, A. Petrone, T. Henderson, D. Ranasinghe, V. G. Zakrzewski, J. Gao, N. Rega, G. Zheng, W. Liang, M. Hada, M. Ehara, K. Toyota, R. Fukuda, J. Hasegawa, M. Ishida, T. Nakajima, Y. Honda, O. Kitao, H. Nakai, T. Vreven, K. Throssell, J. A. Montgomery Jr, J. E. Peralta, F. Ogliaro, M. Bearpark, J. J. Heyd, E. Brothers, K. N. Kudin, V. N. Staroverov,

T. Keith, R. Kobayashi, J. Normand, K. Raghavachari, A. Rendell, J. C. Burant, S. S. Iyengar, J. Tomasi, M. Cossi, J. M. Millam, M. Klene, C. Adamo, R. Cammi, J. W. Ochterski, R. L. Martin, K. Morokuma, O. Farkas, J. B. Foresman and D. J. Fox, *Gaussian 09, revision A.02*, Gaussian, Inc., Wallingford, CT, 2016, p. 645.

13 S. Ramanathan, V. Ponnuswamy, R. Mariappan, K. Nazeer and S. Murugavel, *Elixir Org. Chem.*, 2012, **43**, 6952.

14 M. Peesan, A. Sirivat, P. Supaphol and R. Rujiravanit, *Carbohydr. Polym.*, 2006, **64**, 175.

15 Y. Aysegul, U. Aysegul and B. Venkatr, *Carbohydr. Polym.*, 2009, **75**, 448.

16 R. Karthik and S. Meenakshi, *Chem. Eng. J.*, 2015, **263**, 168.

17 A. Yavuz, A. Uygun and H. Can, *Carbohydr. Res.*, 2011, **346**, 2063.

18 A. Ramaprasad, V. Rao, G. Sanjeev, S. Ramanani and S. Sabharwal, *Synth. Met.*, 2009, **159**, 1983.

19 F. El-Dib, M. Hussein, H. Hefni, G. Eshaq and A. EIMEtwally, *J. Appl. Polym. Sci.*, 2014, **131**, 547.

20 Y. Ismail, S. Shin, K. Shin, S. Yoon, K. Shon, S. Kim and S. Kim, *Sens. Actuators, B*, 2008, **129**, 834.

21 S. Martel-Estrada, C. Martínez-Pérez, J. Chacón-Nava, P. García-Casillas and I. Olivas-Armendariz, *Carbohydr. Polym.*, 2010, **81**, 775.

22 S. Kim, S. Yoom, I. Kim and S. Kim, *J. Appl. Polym. Sci.*, 2004, **91**, 2876.

23 F. Rezaei, N. Tavandashti and A. Zahedi, *Res. Chem. Intermed.*, 2013, **40**, 1233.

24 Z. Zakaria, N. Halim, M. Schleusingen and M. Ahmad, *J. Nanomater.*, 2015, **2015**, 1.

25 S. Imran, Y. Kim, G. Shao, M. Hussain, Y. Choa and H. Kim, *J. Mater. Sci.*, 2014, **49**, 1328.

26 S. Sedaghat, *Int. Nano Lett.*, 2014, **4**, 1.

27 A. Yavuz and A. Gök, *Synth. Met.*, 2007, **157**, 235.

28 M. Ayad, N. Salahuddin, I. Minisy and W. Amer, *Sens. Actuators, B*, 2014, **202**, 144.

29 G. Quartarone, M. Battilana, L. Bonaldo and T. Tortato, *Corros. Sci.*, 2008, **50**, 3467.

30 H. Obayes, G. Alwan, A. Alobaidy, A. Al-Amiery, A. Kadhum and A. Mohamad, *Chem. Cent. J.*, 2014, **8**, 1.

31 H. Lgaz, R. Salghi and S. Jodeh, *Int. J. Corros. Scale Inhib.*, 2016, **5**, 347.

32 H. Gerengi and H. Sahin, *J. Ind. Eng. Chem.*, 2012, **51**, 780.

33 I. Obot, A. Madhankumar, S. Umoren and Z. Gasem, *J. Adhes. Sci. Technol.*, 2015, **29**, 2130.

34 A. Dutta, S. Saha, P. Banerjee and D. Sukul, *Corros. Sci.*, 2015, **98**, 541.

35 B. Mistry and S. Jauhari, *Chem. Eng. Commun.*, 2014, **201**, 961.

36 B. Mistry, D. Kim and S. Jauhari, *Trans. Indian Inst. Met.*, 2016, **69**, 1297.

37 P. Okafor and Y. Zheng, *Corros. Sci.*, 2009, **51**, 850.

38 C. Jeyaprabha, S. Sathiyanarayanan and G. Venkatachari, *J. Appl. Polym. Sci.*, 2006, **101**, 2144.

39 S. Hua, W. Tong, Y. Qiang and H. Rong, *Anti-Corros. Methods Mater.*, 2011, **58**, 111.

40 V. Srivastava and M. Singh, *J. Appl. Electrochem.*, 2010, **40**, 2135.

41 C. Xing, Z. Zhang, L. Yu, L. Zhang and G. Bowmaker, *RSC Adv.*, 2014, **4**, 32718.

42 Y. Sasikumar, A. Adekunle, L. Olasunkanmi, I. Bahadur, R. Baskar, M. Kabanda, I. Obot and E. Ebenso, *J. Mol. Liq.*, 2015, **211**, 105.

43 S. Umoren, I. Obot, A. Madhankumar and Z. Gasem, *J. Adhes. Sci. Technol.*, 2015, **29**, 271.

44 K. Khaled and M. Al-Qahtani, *Mater. Chem. Phys.*, 2009, **113**, 150.

45 M. Gholami, I. Danaee, M. Maddahy and M. RashvandAveiet, *Ind. Eng. Chem. Res.*, 2013, **52**, 14875.

46 J. Syed, S. Tang, H. Lu and X. Meng, *Ind. Eng. Chem. Res.*, 2015, **54**, 2950.

47 Y. Qiang, S. Zhang, B. Tan and S. Chen, *Corros. Sci.*, 2018, **133**, 6.

48 Y. Qiang, S. Zhang, L. Guo, X. Zheng, B. Xiang and S. Chen, *Corros. Sci.*, 2017, **119**, 68.

49 S. Sathiyanarayanan, C. Jeyaprabha and G. Venkatachari, *Mater. Chem. Phys.*, 2008, **107**, 350.

50 M. Lebrini, M. Lagrenée, H. Vezin, M. Traisnel and F. Bentiss, *Corros. Sci.*, 2007, **49**, 2254.

51 R. Geethanjali and S. Subhashini, *J. Food Saf.*, 2015, **33**, 35.

52 H. Xiao, H. Wu and X. Chi, SCE: Grid Environment for Scientific Computing, in *Networks for Grid Applications, GridNet 2008, Lecture Notes of the Institute for Computer Sciences, Social Informatics and Telecommunications Engineering*, ed. P. Vicat-Blance primet, T. Kudoh and J. Mambretti, Springer, Berlin, Heidelberg, 2009, vol. 2.

53 Q. Liao, Z. Yue, D. Yang, Z. Wang, Z. Li, H. Ge and Y. Li, *Corros. Sci.*, 2011, **53**, 1999.

54 K. Khaled, *Appl. Surf. Sci.*, 2006, **252**, 4120.

55 P. Stephens, F. Devlin, C. Chabalowski and M. Frische, *J. Phys. Chem.*, 1994, **98**, 11623.

56 S. Hari Kumar and S. Karthikeyan, *Ind. Eng. Chem. Res.*, 2013, **52**, 7457.

57 Y. Qiang, S. Zhang, S. Yan, X. Zou and S. Chen, *Corros. Sci.*, 2017, **126**, 295.

58 S. H. Yoo, Y. W. Kim, K. Chung, N. K. Kim and J. S. Kim, *Ind. Eng. Chem. Res.*, 2013, **52**, 10880.

59 R. E. Morsi, E. A. Khamis and A. M. Al-Sabagh, *J. Taiwan Inst. Chem. Eng.*, 2016, **60**, 573.

60 I. Ahamad, R. Prasad and M. A. Quraishi, *Corros. Sci.*, 2010, **52**, 1472.